Title

Increasing SERCA function promotes initiation of calcium sparks and breakup of calcium waves

Journal

The Journal of Physiology, 599(13)

ISSN

0022-3751

Authors

Sato, Daisuke

Uchinoumi, Hitoshi

Bers, Donald M

Publication Date

2021-07-01

DOI

10.1113/jp281579

Peer reviewed

HHS Public Access

Author manuscript

J Physiol. Author manuscript; available in PMC 2022 July 01.

Published in final edited form as:

J Physiol. 2021 July ; 599(13): 3267–3278. doi:10.1113/JP281579.

Increasing SERCA function promotes initiation of calcium sparks and breakup of calcium waves

Daisuke Sato[1], **Hitoshi Uchimoumi**[1,2], **Donald M. Bers**[1]

[1] Department of Pharmacology, University of California, Davis School of Medicine

[2]Department of Cardiology, Yamaguchi University School of Medicine

Abstract

Waves of sarcoplasmic reticulum (SR) calcium (Ca) release can cause arrhythmogenic afterdepolarizations in cardiac myocytes. Ca waves propagate when Ca sparks at one Ca release unit (CRUs) recruit new Ca sparks at neighboring CRUs. Under normal conditions, Ca sparks are too small to recruit neighboring Ca sparks where Ca sensitivity is also low. However, under pathological conditions such as a Ca overload or ryanodine receptor (RyR) sensitization, Ca sparks can be larger and propagate more readily as macro-sparks or full Ca waves. Increasing SERCA pump activity promotes SR Ca load, which promotes RyR opening and increases driving force of the Ca release flux from SR to cytosol, promoting Ca waves. However, high SERCA activity can also decrease local cytosolic [Ca] as it approaches the next CRU, thereby reducing wave appearance and propagation. In this study, we use a physiologically detailed model of subcellular Ca cycling and experiments in phospholamban-knockout mice, to show how Ca waves are initiated and propagate and how different conditions contribute to the generation and propagation of Ca waves. We show that reducing diffusive coupling between Ca sparks by increasing SERCA activity prevents Ca waves by reducing [Ca] at the next CRU, as do Ca buffers, low intra-SR Ca diffusion, and distance between CRUs. Increasing SR Ca uptake rate has a biphasic effect on Ca wave propagation, initially it enhances Ca spark probability and amplitude and CRU-coupling, thereby promoting arrhythmogenic Ca waves propagation, but at higher levels SR Ca uptake can abort those arrhythmogenic Ca waves.

Keywords

SERCA; Calcium wave; Calcium spark; Ryanodine receptor; Calcium buffer; Sarcoplasmic reticulum

INTRODUCTION

Cardiac arrhythmia is often triggered by premature ventricular contractions (PVCs), which have been linked to early (EADs) and delayed afterdepolarizations (DADs) (Frazier *et al.*, 1989; Gilmour & Moise, 1996; Nakajima *et al.*, 1997; Akar & Rosenbaum, 2003; Burashnikov & Antzelevitch, 2003; Katra & Laurita, 2005; Rodriguez *et al.*, 2005; Hirose &

Address for correspondence and Proofs: Daisuke Sato, PhD., Department of Pharmacology, University of California, Davis, Genome Building Rm 3503, Davis, CA 95616-8636.

Laurita, 2007; Patterson *et al.*, 2007). One cause of afterdepolarizations is transient inward current (I_{ti}), which is carried primarily by inward sodium-calcium exchanger (NCX) current (I_{NCX}) when intracellular Ca concentration ($[Ca]_i$) is elevated (Tseng & Wit, 1987; January & Fozzard, 1988; Lipp & Pott, 1988; Schlotthauer & Bers, 2000; Verkerk *et al.*, 2001; Voigt *et al.*, 2012). I_{ti} becomes larger when spontaneous Ca releases initiate Ca waves. Under normal (healthy) conditions, Ca sparks are isolated and Ca waves rarely occur (Cheng *et al.*, 1996). However, under diseased conditions such as a Ca overload or ryanodine receptor (RyR) sensitization, Ca sparks recruit new Ca sparks in neighboring Ca release units (CRUs) and propagate as a wave (Cheng *et al.*, 1996; Lukyanenko *et al.*, 1999). As Ca wave amplitude, frequency and propagation rate increase, I_{ti} increases and depolarizes cell membrane. As these afterdepolarizations become larger, they can exceed the threshold of sodium (Na) channel activation and produce triggered action potentials, that at the whole heart level can manifest as premature ventricular contractions (PVCs).

The sarcoplasmic/endoplasmic reticulum calcium ATPase (SERCA) pumps Ca from cytosol to the sarcoplasmic reticulum (SR) and maintains the large [Ca] gradient required for SR Ca release. During excitation-contraction (E-C) coupling SR Ca release amplifies Ca entry through L-type Ca channels. Ca released from the SR and that enters via Ca current (I_{Ca}; in the same cleft region) diffuses into cytosol to activate contraction. For relaxation, Ca ions are mainly removed from cytosol via SERCA or NCX (with tiny amounts removed via sarcolemmal Ca-pump and mitochondrial uniporter)(Bers, 2002). The relative Ca amounts transported by SERCA and NCX varies with species and conditions as determined by various factors such as the number of transporters, cytosolic and intra SR free Ca concentrations ($[Ca]_i$, $[Ca]_{SR}$), $[Na]_i$, membrane voltage, regulation (e.g. by phospholamban; PLN) and temperature. During normal EC coupling, ~70 % of Ca ions returns to the SR and ~25% leaves via NCX in rabbit ventricular myocytes (Bers & Bridge, 1989; Bassani *et al.*, 1994) whereas 92% of Ca ions go back to the SR for rat and mouse ventricular myocytes (Bers & Bridge, 1989; Negretti *et al.*, 1993; Bassani *et al.*, 1994; Li *et al.*, 1998; Bers, 2002).

The CRU is composed of ryanodine receptors (RyR) whose opening is sensitive to both $[Ca]_i$ and $[Ca]_{SR}$ (Gyorke & Gyorke, 1998; Gyorke *et al.*, 2004; Zima *et al.*, 2010; Bers, 2014). Increasing $[Ca]_{SR}$ leads to higher RyR open probability and also increases Ca spark size and duration due to larger driving force for the SR Ca release flux. The refilling speed of SR Ca and the maximum $[Ca]_{SR}$ depend on the SERCA activity vs. the sum of residual leak mediated by RyR and non-RyR mechanisms (Zima *et al.*, 2010; Bers, 2014). When SERCA becomes more active, $[Ca]_{SR}$ increases and thus higher SERCA activity tends to increase both Ca sparks and Ca waves. However, recent experimental and clinical studies show that increasing SERCA activity prevents Ca waves and arrhythmia (Huser *et al.*, 1998; del Monte *et al.*, 2004; Kawase & Hajjar, 2008; Prunier *et al.*, 2008; Lipskaia *et al.*, 2010; Jessup *et al.*, 2011; Bai *et al.*, 2013). One explanation for this could be that the increasing SERCA activity limits the propagation of Ca waves by reducing the spatiotemporal spread of local $[Ca]_i$ release, thereby preventing spark activation at adjacent CRUs. In this study, we use physiologically detailed computational models of the subcellular Ca cycling and experimental validation in using PLN-KO mice, showing how increasing SERCA activity can both promote and reduce the propensity of Ca wave propagation in various conditions.

MATERIALS AND METHODS

Mathematical model

In order to simulate realistic Ca sparks and waves, we use a modified version of a physiologically detailed model of a rabbit ventricular myocyte used in our previous studies (Sato & Bers, 2011; Sato *et al.*, 2012). This model is based on models by Shannon *et al.* (Shannon *et al.*, 2004) and Restrepo *et al* (Restrepo *et al.*, 2008). Fig 1 is the schematic illustration of the model. Near each CRU there are 5 Ca compartments; bulk cytosolic Ca ($[Ca]_i$), submembrane Ca ($[Ca]_{sm}$), cleft space Ca ($[Ca]_{Cleft}$), network SR Ca ($[Ca]_{SRN}$), and junctional SR Ca ($[Ca]_{JSR}$). CRUs are also coupled by Ca diffusion in cytosol and the network SR. The major difference from the previous versions of this model is Ca diffusion in submembrane space. The $[Ca]_{sm}$ diffusion is primarily in a transverse vs. longitudinal direction, based on the fact that most CRUs are along transverse tubules (T-tubules) that define the internal submembrane space. The model has 4-state RyR channels, which are sensitive to both cytosolic Ca ($[Ca]_i$) and SR Ca ($[Ca]_{SR}$). No Ca waves are observed with normal (healthy) baseline rabbit parameters. Therefore, we increased RyR sensitivity to Ca to mimic diseased conditions such as catecholaminergic polymorphic ventricular tachycardia (CPVT) mutations. There are 19,305 CRUs (65×27×11) in the cell. One CRU contains 100 RyRs and thus there are 1,930,500 RyRs in the cell. Geometrical parameters such as the distance between CRUs and diffusion constants, for longitudinal direction and transverse direction are different based on experimental measurements. The cell model is a cuboid (65×27×11 CRUs). In order to avoid geometrical effects of the cell shape, 50×3×3 (longitudinal × transverse × transverse) and 3×50×3 cell structures are used to compare propagations of longitudinal and transverse waves. SERCA pumps are distributed equally over the cell. The maximum transport rate of the SERCA pump (v_{up}) is varied to mimic SERCA overexpression. Ca affinity of the SERCA pump (K_d) is also varied to mimic β-adrenergic stimulation. All parameters are given in the appendix. The program codes are written in C++ and simulated in a High-Performance Computing cluster (24 nodes, Intel Xeon E3–1270, 3.4GHz, 32GB RAM) and Amazon Web Services.

In a quiescent cell, $[Ca]_i$ is independent of the SERCA activity at the steady state. In other words, the SERCA activity does not have influence for $[Ca]_i$ at the steady state and $[Ca]_i$ is solely determined by the balance between transmembrane fluxes. On the other hand, $[Ca]_{SR}$ is determined by the balance between the SERCA uptake flux and SR Ca leak fluxes. The SERCA pump is given by

$$I_{up} = v_{up}\left(\left(\frac{[\mathrm{Ca}]_i}{k_{\mathrm{up}}}\right)^H - \left(\frac{[\mathrm{Ca}]_{\mathrm{SR}}}{k_{\mathrm{SR}}}\right)^H\right)/\left(1 + \left(\frac{[\mathrm{Ca}]_i}{k_{\mathrm{up}}}\right)^H\right).$$

$[Ca]_{SR}$-dependent SR Ca leak via RyR is given by

$$I_r = J_{max}\frac{P_o([\mathrm{Ca}]_{\mathrm{JSR}} - [\mathrm{Ca}]_{\mathrm{cleft}})}{v_p}.$$

The RyR channel gating model is a four-state Markovian model regulated by $[Ca]_{Cleft}$ and $[Ca]_{jSR}$. Each RyR opens independently and stochastically. As shown in our previous studies (Sato & Bers, 2011; Sato *et al.*, 2012; Xie *et al.*, 2019), several changes to the Restrepo et al model were made, including:

1. The rates from the closed state to the open state

$$k_{12} = \frac{K_u[\mathrm{Ca}]^2_{\mathrm{Cleft}}}{K^2_{\mathrm{cp}} + [\mathrm{Ca}]^2_{\mathrm{Cleft}}} + w,$$

$$k_{43} = \frac{K_b[\mathrm{Ca}]^2_{\mathrm{Cleft}}}{K^2_{\mathrm{cp}} + [\mathrm{Ca}]^2_{\mathrm{Cleft}}} + w,$$

where k_{12} is the rate from state 1 to state 2, k_{43} is the sate from state 4 to state 3, Ku, K_{cp},K_b and w are constants.

2. The rates from the open state to the closed state to fit the experimental observation of the mean open times (0.7~1.9 ms) (Györke & Györke, 1998)

$$k_{21} = 0.5\ \mathrm{ms}^{-1},\ k_{34} = 3.3\ \mathrm{ms}^{-1}$$

The other equations are the same as that used by Restrepo et al.

$$k_{14} = \frac{\widehat{M}([\mathrm{Ca}]_{\mathrm{jSR}})\tau_b^{-1}B_{CSQN}}{B^0_{CSQN}},$$

$$k_{23} = \frac{\widehat{M}([\mathrm{Ca}]_{\mathrm{jSR}})\tau_b^{-1}B_{CSQN}}{B^0_{CSQN}},$$

$$k_{41} = \frac{1}{\tau_u},$$

$$k_{32} = \frac{k_{41}k_{12}}{k_{43}}.$$

The total SR Ca content ($[Ca]_{SRT}$) is controlled by the balance of net SR Ca uptake by SERCA (above) and $[Ca]_{SR}$-dependent SR Ca leak via RyR (J_{RyR}) (above) and non-RyR leak (J_{lk}) as $d[Ca]_{SRT}/dt = I_{up} - J_{RyR} - J_{lk}$ (see appendix). Notably, when there is no SR Ca leak, $[Ca]_{SR}$ becomes the maximum value (thermodynamic limit) and given by

$$[\mathrm{Ca}]_{\mathrm{SR}} = \left(\frac{k_{\mathrm{SR}}}{k_{\mathrm{up}}}\right)[\mathrm{Ca}]_i .$$

This is independent of the SERCA pump strength (v_{up}). We use these $[Ca]_i$ and $[Ca]_{SR}$ as initial conditions and also allow the model to relax to steady state. This allows us to investigate the effect of SERCA overexpression, which changes the SERCA pump strength (v_{up}), and the effect of SR Ca load separately. Of note, we do not use the complex array of sarcolemmal channels and transporters to study intrinsic SR Ca handling in a focal manner.

Ethical approval

All animal protocols were performed in accordance with NIH guidelines and approved by the UC Davis Institutional Animal Care and Use Committee (IACUC). PLN knockout (PLN-KO) mice and wild type littermates were generously provided by Dr. E.G. Kranias (University of Cincinnati, OH), an animal model described in their previous work (Luo *et al.*, 1994). Mice were group housed with *ad libitum* access to food and water and maintained at 22°C on a 12 h:12 h light–dark cycle. The authors understand the ethical principles under which *The Journal of Physiology* operates and declare that our work complies with its animal ethics checklist.

Mouse cardiac ventricular myocyte isolation

Single ventricular myocytes were enzymatically isolated as previously described from hearts of PLN-KO mice.(Li *et al.*, 2002) Briefly, after anesthesia (isoflurane, 5%), mice were anticoagulated with intraperitoneal injection of heparin (8000 units/kg body weight). Hearts were excised and retrograde perfused on constant flow Langendorff apparatus (4 min, 37°C) with the Ca-free normal Tyrode (NT) solution, gassed with 100% O_2. Then, ventricular myocytes were digested by Liberase TM (0.075 mg/mL, Roche) and Trypsin (0.0138%, Gibco). Ventricular myocytes were dispersed mechanically and filtered through a nylon mesh and allowed to sediment for 10 min. The sedimentation is repeated three times every 10 min, while [Ca] (mmol/L) was increased stepwise, from 0.125 to 0.25 through 0.5. Finally, ventricular myocytes were kept in a 0.5 mmol/L [Ca] NT solution at room temperature.

Confocal Ca^{2+} Imaging in Intact Myocytes

Fluo-4 AM (10 μmol/L, Molecular Probes®) was loaded into intact myocytes for 10 min in NT solution (in mmol/L): NaCl 140, KCl 4, $MgCl_2$ 1, $CaCl_2$ 1, glucose 10, HEPES 5, pH 7.4; then incubated for 30 min to allow for de-esterification. The $[Ca]_o$ was increased stepwise from 1 to 3, and 6 mM to induce spontaneous release (Bai *et al.*, 2013). Ca events were recorded with 6 mM $[Ca]_o$ NT solution. Ca events were recorded at room temperature using a confocal microscope (Bio-Rad Radiance 2100 MP, 40× objective) with fluorescence excitation set at 488 nm with emission collected at wavelengths greater than 500 nm.

Statistics

Data were expressed as mean ± SD, and significance was evaluated using Student's t-test or one-way ANOVA. $p<0.05$ was considered statistically significant.

RESULTS

Effects of $[Ca]_{SR}$, $[Ca]_i$ and SERCA function alone on Ca wave Propagation

RyR gating is sensitive to $[Ca]_i$ and $[Ca]_{SR}$. The open probability of a single RyR channel is increasing function of $[Ca]_i$ and $[Ca]_{SR}$ (Fig 2A). In the cell, RyRs are clustered in CRUs, within which RyRs interact nonlinearly through $[Ca]_{Cleft}$. When a single RyR opens, the elevation of local $[Ca]_{Cleft}$ recruits openings of other RyRs within the CRU and the frequency of Ca sparks depends steeply on $[Ca]_{Cleft}$ and $[Ca]_{SR}$ (Fig 2B). The increase of Ca spark frequency saturates since the recovery of RyRs takes several hundred milliseconds (which depends on the refilling rate of $[Ca]_{SR}$ and intrinsic properties of the channel) and RyRs must recover before the next Ca spark occurs. Ca waves propagate when Ca spark-driven Ca flux raises local $[Ca]_i$ and $[Ca]_{Cleft}$ sufficiently at neighboring CRUs to trigger a Ca spark. We measured this probability of Ca spark propagation to an adjacent CRU when inducing a first Ca spark by setting 5 RyRs open in either the longitudinal (Fig 2C) or transverse direction (Fig 2D). We use 3 RyRs opening at that second CRU as a threshold of Ca spark occurrence. Since the CRUs are more closely spaced transversely, Ca sparks propagate more easily than in the longitudinal direction. In this simulation, there was only one Ca spark to initiate the new Ca spark whereas during Ca waves, a cluster of Ca sparks supply large amount of Ca to initiate new Ca sparks. Therefore, in this simulation, relatively higher $[Ca]_{SR}$ was required to initiate new Ca sparks.

Transition from isolated Ca sparks to Ca waves occurs as myocytes load with Ca. In Fig 3, we started with moderate [Ca] (relatively low [Ca] for Ca waves; $[Ca]_{SR}$=1.6 mM, $[Ca]_i$=0.1 μM). In this case, Ca releases from the SR generated only isolated Ca sparks (Fig 3A). The size of Ca sparks was small compared to the separation between CRUs and Ca sparks could not recruit additional neighboring sparks. There was also invisible non-spark leak (Ca quarks; <3 RyR openings). When [Ca] is increased to $[Ca]_{SR}$=1.9 mM and $[Ca]_i$=0.15 μM, Ca sparks were able to initiate new Ca sparks in neighboring CRUs. Ca waves propagated partially in space. These we call macro sparks if only a few Ca sparks are involved or 'mini waves' if the wave propagates, at least, several CRUs. This happened more often in a transverse direction (Fig 3B). When [Ca] was high enough ($[Ca]_{SR}$=2.5 mM and $[Ca]_i$=0.2 μM), multiple Ca waves occurred at different locations and they propagated in both longitudinal and transverse directions.

How do structural differences in longitudinal and transverse directions affect Ca wave propagation? For Ca wave propagation, a Ca spark must recruit new Ca sparks (fire-diffuse-fire) at the neighboring CRUs. We plotted the peak $[Ca]_i$ at the nearest CRU after the first Ca spark occurred, as a function of the SERCA pump strength (v_{up}: Fig 4A & B). We indicate that at 35°C the basal normal v_{up} (in μM/ms) is expected to be 0.212 in rabbit, 0.535 in rat and 0.85 in mouse and can be increased by PLN-KO or PKA activation (Li *et al.*, 1998; Bers, 2001). Since SERCA removes Ca from the cytosol at all points between the 2 CRUs, it

reduces $[Ca]_i$ at both the first spark site and its neighbors. Therefore, if initial $[Ca]_i$ and $[Ca]_{SR}$ are the same, which ensures the same state of RyRs and driving force from SR to cytosol, as SERCA pumps become more active, the local $[Ca]_i$ at the neighboring site becomes smaller and reduces the probability of new Ca sparks at that CRU. We measured probability of whole cell Ca waves when SERCA strength was varied, including longitudinal waves and transverse waves. For longitudinal waves, we used 50×3×3 (longitudinal × transverse × transverse) structure and Ca waves were initiated by stimulating the 45 (5×3×3) leftmost CRUs. To assess transverse waves, we used 3×50×3 (longitudinal × transverse × transverse) structure and Ca waves were initiated by stimulating the 45 (3×5×3) leftmost CRUs. Ca wave propagation was progressively suppressed as SR Ca uptake increases (Fig 4C–D), more dramatically in the longitudinal vs. transverse direction.

Induction of Ca waves depends biphasically on SERCA activity

We show that higher SERCA pump activity suppresses Ca wave propagation (at any fixed $[Ca]_{SR}$; Fig 4), but also that increased SERCA activity tend to increase $[Ca]_{SR}$ which, by itself, promotes Ca sparks and waves (Fig 2). So, how do these opposing effects interact dynamically when the system is allowed to relax to a steady state? Fig 5D shows average $[Ca]_{SR}$ vs. SERCA pump strength (v_{up}) at the steady state (Fig 5D right axis). The higher SERCA pump activity promotes RyR recovery, Ca sparks and raises the driving force for the SR Ca releases, but has a biphasic changes in wave frequency (three cases, depending on v_{up}). At lower SERCA function, Ca waves rarely occur due to lower $[Ca]_{SR}$ which limits Ca spark frequency, amplitude and RyR sensitivity (Fig 5A). At intermediate SERCA activity, the increase in Ca spark frequency, amplitude and sensitivity progressive increases wave frequently (Fig 5B and peak in Fig 5D). Beyond that point, further increase in SERCA function predominantly suppress wave frequency (as in Fig 4C–D). This indicates that the reuptake-dependent curtailment of cytosolic Ca diffusion from an active CRU to any neighboring CRU suppresses propagation, despite a continued increase in Ca spark frequency and local amplitude at the active CRU (Fig 5C). That is, at very high SERCA v_{up}, Ca wave cannot propagate due to fast removal of $[Ca]_i$ before it gets to the next CRU. However, Ca sparks occur more frequently. Thus, there is a window of SERCA strength where Ca wave are promoted (Fig 5D). Fig 5C indeed shows a greatly increased number of release events that are considerably more restricted in propagation (macro-sparks and mini-waves) with very few long propagating waves. A salient point here is that large and fast propagating Ca waves will cause larger and more synchronized inward $I_{NCX,}$ as shown in Fig 5B, which is in the range that can trigger action potentials (Schlotthauer & Bers, 2000) and thus have arrhythmogenic impact.

Increased Ca buffering (e.g. with EGTA) has been used by many groups to suppress Ca waves, while still measuring Ca sparks. That can be pragmatic when using Ca spark frequency to assess SR Ca leak, where occasional Ca waves can reduce $[Ca]_{SR}$ cause reduced $[Ca]_{SR}$ and temporarily suppress Ca sparks. Fig 6A–B shows how increasing Ca buffering also suppresses Ca wave propagation, especially in the longitudinal direction (as with increasing SERCA). If we consider increased SERCA as a spatial buffer for $[Ca]_i$, it makes sense that, like EGTA, it suppresses Ca wave propagation. However, the EGTA effect

is monotonic suppression, because it does not increase $[Ca]_{SR}$ the way SERCA enhancement does to create a window of propagating wave propensity.

We also explored the effect of slowing Ca diffusion in the network SR, which Fig 6C–D shows can promote Ca waves. A typical Ca diffusion constant in the network SR is 60 $\mu m^2/s$ (indicated with a triangle in the figures) (Wu & Bers, 2006; Picht *et al.*, 2011; Bers & Shannon, 2013). We infer that this effect is because if intra-SR diffusion is extremely fast, the local $[Ca]_{SR}$ at the nearest CRU will be significantly depleted, resulting in reduced RyR sensitivity and Ca driving force through the RyRs in that junction. Conversely, with ultra-slow intra-SR diffusion, the neighboring CRU will have the maximal $[Ca]_{SR}$ at the time the wave of cytosolic Ca arrives –making RyRs more sensitive and able to produce larger Ca release flux to drive further propagation. Thus, increased $[Ca]_i$ buffering and fast intra-SR diffusion suppress Ca wave propagation.

Direct test of SERCA functional effects on Ca waves in intact ventricular myocytes

The high SERCA effect in Fig 5C, showing the abortion of propagated waves at high $[Ca]_{SR}$ is reminiscent of prior measurements in PLN-KO mice which have very high SERCA function (Huser *et al.*, 1998; Bai *et al.*, 2013). To test whether the biphasic effect of graded SERCA function on propagating Ca wave frequency in Fig 5D is apparent in live ventricular myocytes we used isolated intact myocytes from PLN-KO mice, which have perhaps the highest basal SERCA activity of any native cardiac myocyte (Li *et al.*, 1998). To induce Ca overload and robust Ca wave activity we raised $[Ca]_o$ from 1 to at least 3 mM.

Figure 7A shows line scan confocal $[Ca]_i$ imaging in a PLN-KO myocyte. At this initial time point (0 min) the myocyte exhibits many abortive mini-waves (Ca Waves that do not propagate the full myocyte length), but few waves that propagate through the full-cell. Then to gradually inhibit SERCA activity we added 0.3 μM cyclopiazonic acid (CPA, a selective SERCA inhibitor) and monitored Ca waves every 2 min. After 2 min exposure of CPA, the number of full propagated (cell-wide) Ca waves increased to a maximum at 2 min (Fig 7A–B) and as more SERCA pumps were progressively blocked the absolute frequency of waves decreased, but most propagated through the entire myocyte length. Indeed, as SERCA became more completely inhibited (at 8–16 min), the wave frequency declined (Fig 7B) as did the amplitude (from 4.08 ± 0.20 at 4 min to 2.17 ± 0.26 at 16 min), consistent with the expected progressive decline in $[Ca]_{SR}$.

We can infer the relative SERCA activity during the CPA exposure by measuring the time constant (τ) of $[Ca]_i$ decline wave during each wave (at any location). Fig 7C shows the measured τ of $[Ca]_i$ as a function of CPA exposure time as mean tau rises from 82 to 311 ms. The inverse of this τ gives a rate constant for $[Ca]_i$ decline, which falls from 12.2 s^{-1} at 0 min to 3.2 s^{-1} at 16 min (Fig 7D). If we correct these rate constants by the 5% contribution of non-SERCA transporters to $[Ca]_i$ decline in the PLN-KO myocyte under control conditions (Li *et al.*, 1998) we can translate the SERCA-dependent uptake rate, as a percent of the maximal SERCA rate at baseline (V_{max}) for each time after CPA addition. (Fig 7D right ordinate scale). That allows us to plot the experimental wave frequency results as a function of maximal SERCA function (Fig 7E), for comparison with the model predictions in Fig 5D. Overall, the same biphasic response of fully-propagating wave frequency to

increasing SERCA function is seen in both curves. That is, there are few waves at low SERCA activity, progressive more as SERCA activity rises, up to a peak, after which the Ca waves are more often aborted and fail to propagate effectively at the highest SERCA function level. While the experimental curve peak is a bit more right-shifted, it shows that a further 20% decrease in SERCA from the peak wave frequency suffices to prevent SERCA from aborting Ca waves.

DISCUSSION

Ca waves propagate when Ca sparks recruit new Ca sparks in neighboring CRUs. This is called fire-diffuse-fire model of Ca wave propagation (Dawson *et al.*, 1999) and implies that diffusion, in other words, coupling between Ca sparks has a crucial role in the propagation as well as the Ca spark itself (‘fire’ in the fire-diffuse-fire model). The properties such as frequency, size, and duration, of Ca spark are substantially influenced by [Ca]. Previous studies show that stochastic openings of RyRs cause non-spark SR Ca leak (Ca quarks) when SR Ca load is low and steeply leads to Ca sparks as SR Ca load becomes higher (Zima *et al.*, 2010; Sato & Bers, 2011; Williams *et al.*, 2011; Bers, 2014). Further Ca loading or overloading promotes a transition from isolated Ca sparks to Ca waves occurs in the cell (Cheng *et al.*, 1996). If the SERCA strength and Ca diffusion are unchanged, higher $[Ca]_{SR}$ promotes Ca waves. This is simply understood as follows. At the single channel level, the opening of RyRs is sensitive to $[Ca]_i$ and $[Ca]_{SR}$ (Gyorke & Gyorke, 1998). Open probability becomes higher as $[Ca]_i$ and $[Ca]_{SR}$ become higher (Fig 2A). At the CRU level, more frequent Ca sparks are observed as $[Ca]_{SR}$ become higher, not only due to higher open probability of RyRs but also due to higher driving force and positive feedback process of CICR (Fig 2B). As $[Ca]_{SR}$ becomes higher, Ca spark becomes larger and longer. This causes higher $[Ca]_i$ at the neighbor and initiate new sparks (Fig 4A–B).

In this study we focused more on diffusive coupling in the fire-diffuse-fire model enabling strong Ca wave propagation that is proarrhythmic. As Ca is loaded into the cell, we show how isolated Ca sparks become macro-sparks by recruiting new Ca sparks from neighboring CRUs. First, we examined the effects of initially fixing $[Ca]_i$ and $[Ca]_{SR}$ (Fig 2–3) in order to keep the same RyR states and driving force for the SR Ca release. Then, we varied the SERCA strength, revealing the intrinsic effect of more active SERCA to suppress wave propagation (Fig 4C–D), effectively reducing coupling between CRUs because SERCA progressive reduces local $[Ca]_i$ in the space between CRUs. When we allow the system to relax to steady state it determines its own $[Ca]_{SR}$ level and reveals the biphasic effect of SERCA activity on Ca waves (Fig 5).

$[Ca]_{SR}$ is determined by the balance between SR Ca leak and reuptake by SERCA. Thus, increasing SERCA activity increases $[Ca]_{SR}$. Therefore, where the effect of increasing $[Ca]_{SR}$ on Ca wave dominates, increasing SERCA activity promotes Ca waves. On the other hand, if the effect of decreasing $[Ca]_i$ between CRUs dominates, waves are suppressed. In other words, increasing SERCA promotes ‘fire’ but suppresses ‘diffuse’ in the fire-diffuse-fire model. Therefore, increasing SERCA-pump function has a biphasic effect on propensity of arrhythmogenic Ca waves, but a monotonic effect to increase Ca spark frequency and amplitude.

Here, we varied the maximum transport rate of SERCA (v_{up}) to mimic SERCA overexpression. Increasing SERCA activity by enhancing Ca affinity (reducing k_d), which mimics β-adrenergic stimulation, PLN phosphorylation or PLN-KO also reveals an analogous biphasic effect on wave propagation (Fig 8A). Increasing RyR cluster size reduces SR Ca load, but increase Ca spark frequency (Galice *et al.*, 2018; Xie *et al.*, 2019). When RyR cluster size was doubled in our model, the wave frequency was increased, but then declined at higher SERCA activity (Fig 8B). Thus, this biphasic effect of SERCA enhancement on Ca wave propagation seems to be a general phenomenon.

Our experimental results using PLN-KO mice support our simulation results (Fig 7). We note that wild type mice did not readily exhibit the biphasic effect (Fig 8C). That is, progressive inhibition of SERCA caused a monotonic decrease in Ca waves. It may thus be that the protective effect of wave suppression by SERCA enhancement can only be reached under extremely high SERCA activity, such that the more arrhythmogenic consequence is more dominant over most of the physiological rage of SERCA enhancement.

Nevertheless, while some studies show that reducing SERCA expression reduces Ca waves (Stokke *et al.*, 2010), Davia *et al.* showed that SERCA overexpression reduces aftercontractions (Davia *et al.*, 2001). A recent study by Bai *et al.* showed that PLN-KO in a CPVT RyR2 mutant mouse have less frequent Ca waves but more frequent Ca sparks compared to CPVT mutant mice (Bai *et al.*, 2013). This RyR2 causes substantial increases in Ca sparks (as may also occur in other pathological states) which would amplify the amount of SR Ca release for a given $[Ca]_{SR}$ and $[Ca]_i$, increasing waves analogous to the doubling of cluster size (Fig 8B). This emphasizes that enhancing SERCA function may also limit arrhythmogenic propagating waves that result from sensitized RyR2, whether from genetic CPVT-linked mutations or pathological states like heart failure, chronic Ca/calmodulin-dependent protein kinase II (CaMKII) activation or oxidative stress.

Another important point in our study is differences of Ca wave propagation in longitudinal and transverse directions. In ventricular myocytes, CRUs locate primarily along T-tubules with some under the surface sarcolemma and only rare RyRs in network SR. Along T-tubules CRUs are typically only 0.5–1 μm, vs. the roughly 2 μm longitudinal sarcomeric spacing. We show how much more robust transverse CRU coupling is versus longitudinal coupling, but for a more arrhythmogenic cell-wide Ca wave longitudinal coupling is essential. One can picture then how transverse CRU coupling is easier to achieve (Fig 3), but that recruitment of several transverse CRUs can provide the stronger Ca source that drives longitudinal propagation.

It has shown that sensitization of RyR ahead of Ca wave front may promote Ca waves (Keller *et al.*, 2007; Ramay *et al.*, 2010; Maxwell & Blatter, 2012) presumably by SERCA-dependent uptake between CRUs that raises local $[Ca]_{SR}$ at the next CRU. We show here that as Ca diffusion in the network SR is decreased, Ca waves propagate more readily (Fig 6C–D), because it prevents depletion of $[Ca]_{SR}$ at that next CRU that could be caused by depletion at the first CRU (if intra-SR diffusion is fast). Picht *et al.* measured the spatiotemporal spread of intra-SR depletion during individual Ca sparks (Picht *et al.*, 2011). While $[Ca]_{SR}$ depletion 0.8 μm from the initiating spark CRU was similar in transverse and

longitudinal directions (roughly half of that at the releasing CRU), the depletion impact would be greater in the transverse direction where a neighboring CRU is at that 0.8 μm range. There was substantial variation in how diffusionally connected a particular CRU was, but for the intra-SR diffusion coefficients that matched the data, there would typically be very little depletion at a longitudinal CRU that is 2 μm away from the active CRU.

In conclusion, we have shown how increased SERCA function can both promote and suppress Ca wave propagation. For modest amounts of SERCA increase, the promotion of arrhythmogenic Ca waves predominates, but even higher SERCA enhancement can limit that Ca wave propagation. This is because enhancing SERCA activity increases SR Ca load, which promotes Ca sparks and propagation as waves, but the ability of high SERCA activity can prevent Ca from one CRU from reaching and activating a next CRU. Therefore, enhancing SERCA activity always leads to the higher Ca spark frequency but under certain conditions can lower Ca wave propensity. Lowering SERCA activities also reduces the propensity of Ca wave propagation, but at the potential cost of lower Ca transients and cardiac contraction.

Supplementary Material

Refer to Web version on PubMed Central for supplementary material.

ACKNOWLEDGEMENTS

Supported by National Institutes of Health grant R00-HL111334 (DS), R01-HL149349 (D.S. & DMB), P01-HL141084 (DMB & DS), and R01-HL092097 (DMB), American Heart Association Grant-in-Aid 16GRNT31300018 (DS) and Amazon AWS Cloud Credits for Research (DS).

REFERENCES

Akar FG & Rosenbaum DS. (2003). Transmural electrophysiological heterogeneities underlying arrhythmogenesis in heart failure. Circ Res 93, 638–645. [PubMed: 12933704]

Bai Y, Jones PP, Guo J, Zhong X, Clark RB, Zhou Q, Wang R, Vallmitjana A, Benitez R, Hove-Madsen L, Semeniuk L, Guo A, Song LS, Duff HJ & Chen SR. (2013). Phospholamban knockout breaks arrhythmogenic Ca^{2+} waves and suppresses catecholaminergic polymorphic ventricular tachycardia in mice. Circ Res 113, 517–526. [PubMed: 23856523]

Bassani JW, Bassani RA & Bers DM. (1994). Relaxation in rabbit and rat cardiac cells: species-dependent differences in cellular mechanisms. J Physiol 476, 279–293. [PubMed: 8046643]

Bers D (2001). Excitation-Contraction Coupling and Cardiac Contractile Force, vol. 237.

Bers DM. (2002). Cardiac excitation-contraction coupling. Nature 415, 198–205. [PubMed: 11805843]

Bers DM. (2014). Cardiac sarcoplasmic reticulum calcium leak: basis and roles in cardiac dysfunction. Annu Rev Physiol 76, 107–127. [PubMed: 24245942]

Bers DM & Bridge JH. (1989). Relaxation of rabbit ventricular muscle by Na-Ca exchange and sarcoplasmic reticulum calcium pump. Ryanodine and voltage sensitivity. Circ Res 65, 334–342. [PubMed: 2546695]

Bers DM & Shannon TR. (2013). Calcium movements inside the sarcoplasmic reticulum of cardiac myocytes. J Mol Cell Cardiol 58, 59–66. [PubMed: 23321551]

Burashnikov A & Antzelevitch C. (2003). Reinduction of atrial fibrillation immediately after termination of the arrhythmia is mediated by late phase 3 early afterdepolarization-induced triggered activity. Circulation 107, 2355–2360. [PubMed: 12695296]

Cheng H, Lederer MR, Lederer WJ & Cannell MB. (1996). Calcium sparks and $[Ca^{2+}]i$ waves in cardiac myocytes. Am J Physiol 270, C148–159. [PubMed: 8772440]

Davia K, Bernobich E, Ranu HK, del Monte F, Terracciano CM, MacLeod KT, Adamson DL, Chaudhri B, Hajjar RJ & Harding SE. (2001). SERCA2A overexpression decreases the incidence of aftercontractions in adult rabbit ventricular myocytes. J Mol Cell Cardiol 33, 1005–1015. [PubMed: 11343422]

Dawson SP, Keizer J & Pearson JE. (1999). Fire-diffuse-fire model of dynamics of intracellular calcium waves. Proc Natl Acad Sci U S A 96, 6060–6063. [PubMed: 10339541]

del Monte F, Lebeche D, Guerrero JL, Tsuji T, Doye AA, Gwathmey JK & Hajjar RJ. (2004). Abrogation of ventricular arrhythmias in a model of ischemia and reperfusion by targeting myocardial calcium cycling. Proc Natl Acad Sci U S A 101, 5622–5627. [PubMed: 15044708]

Frazier DW, Wolf PD, Wharton JM, Tang AS, Smith WM & Ideker RE. (1989). Stimulus-induced critical point. Mechanism for electrical initiation of reentry in normal canine myocardium. J Clin Invest 83, 1039–1052. [PubMed: 2921316]

Galice S, Xie Y, Yang Y, Sato D & Bers DM. (2018). Size Matters: Ryanodine Receptor Cluster Size Affects Arrhythmogenic Sarcoplasmic Reticulum Calcium Release. J Am Heart Assoc 7.

Gilmour RF Jr. & Moise NS. (1996). Triggered activity as a mechanism for inherited ventricular arrhythmias in German shepherd Dogs. J Am Coll Cardiol 27, 1526–1533. [PubMed: 8626969]

Gyorke I & Gyorke S. (1998). Regulation of the cardiac ryanodine receptor channel by luminal Ca^{2+} involves luminal Ca^{2+} sensing sites. Biophys J 75, 2801–2810. [PubMed: 9826602]

Gyorke I, Hester N, Jones LR & Gyorke S. (2004). The role of calsequestrin, triadin, and junctin in conferring cardiac ryanodine receptor responsiveness to luminal calcium. Biophys J 86, 2121–2128. [PubMed: 15041652]

Hirose M & Laurita KR. (2007). Calcium-mediated triggered activity is an underlying cellular mechanism of ectopy originating from the pulmonary vein in dogs. Am J Physiol Heart Circ Physiol 292, H1861–1867. [PubMed: 17158650]

Huser J, Bers DM & Blatter LA. (1998). Subcellular properties of $[Ca^{2+}]$i transients in phospholamban-deficient mouse ventricular cells. American J Physiol 274, H1800–1811.

January CT & Fozzard HA. (1988). Delayed afterdepolarizations in heart muscle: mechanisms and relevance. Pharmacol Rev 40, 219–227. [PubMed: 3065793]

Jessup M, Greenberg B, Mancini D, Cappola T, Pauly DF, Jaski B, Yaroshinsky A, Zsebo KM, Dittrich H, Hajjar RJ & Calcium Upregulation by Percutaneous Administration of Gene Therapy in Cardiac Disease I. (2011). Calcium Upregulation by Percutaneous Administration of Gene Therapy in Cardiac Disease (CUPID): a phase 2 trial of intracoronary gene therapy of sarcoplasmic reticulum Ca2+-ATPase in patients with advanced heart failure. Circulation 124, 304–313. [PubMed: 21709064]

Katra RP & Laurita KR. (2005). Cellular mechanism of calcium-mediated triggered activity in the heart. Circ Res 96, 535–542. [PubMed: 15718502]

Kawase Y & Hajjar RJ. (2008). The cardiac sarcoplasmic/endoplasmic reticulum calcium ATPase: a potent target for cardiovascular diseases. Nat Clin Pract Cardiovasc Med 5, 554–565. [PubMed: 18665137]

Keller M, Kao JP, Egger M & Niggli E. (2007). Calcium waves driven by “sensitization” wave-fronts. Cardiovasc Res 74, 39–45. [PubMed: 17336953]

Li L, Chu G, Kranias EG & Bers DM. (1998). Cardiac myocyte calcium transport in phospholamban knockout mouse: relaxation and endogenous CaMKII effects. Am J Physiol 274, H1335–1347. [PubMed: 9575939]

Li Y, Kranias EG, Mignery GA & Bers DM. (2002). Protein kinase A phosphorylation of the ryanodine receptor does not affect calcium sparks in mouse ventricular myocytes. Circ Res 90, 309–316. [PubMed: 11861420]

Lipp P & Pott L. (1988). Transient inward current in guinea-pig atrial myocytes reflects a change of sodium-calcium exchange current. J Physiol 397, 601–630. [PubMed: 2457703]

Lipskaia L, Chemaly ER, Hadri L, Lompre AM & Hajjar RJ. (2010). Sarcoplasmic reticulum Ca^{2+} ATPase as a therapeutic target for heart failure. Expert Opin Biol Ther 10, 29–41. [PubMed: 20078230]

Lukyanenko V, Subramanian S, Gyorke I, Wiesner TF & Gyorke S. (1999). The role of luminal Ca^{2+} in the generation of Ca^{2+} waves in rat ventricular myocytes. J Physiol 518 (Pt 1), 173–186. [PubMed: 10373699]

Luo W, Grupp IL, Harrer J, Ponniah S, Grupp G, Duffy JJ, Doetschman T & Kranias EG. (1994). Targeted ablation of the phospholamban gene is associated with markedly enhanced myocardial contractility and loss of beta-agonist stimulation. Circ Res 75, 401–409. [PubMed: 8062415]

Maxwell JT & Blatter LA. (2012). Facilitation of cytosolic calcium wave propagation by local calcium uptake into the sarcoplasmic reticulum in cardiac myocytes. J Physiol 590, 6037–6045. [PubMed: 22988145]

Nakajima T, Kaneko Y, Taniguchi Y, Hayashi K, Takizawa T, Suzuki T & Nagai R. (1997). The mechanism of catecholaminergic polymorphic ventricular tachycardia may be triggered activity due to delayed afterdepolarization. Eur Heart J 18, 530–531. [PubMed: 9076398]

Negretti N, O'Neill SC & Eisner DA. (1993). The relative contributions of different intracellular and sarcolemmal systems to relaxation in rat ventricular myocytes. Cardiovasc Res 27, 1826–1830. [PubMed: 8275530]

Patterson E, Jackman WM, Beckman KJ, Lazzara R, Lockwood D, Scherlag BJ, Wu R & Po S. (2007). Spontaneous pulmonary vein firing in man: relationship to tachycardia-pause early afterdepolarizations and triggered arrhythmia in canine pulmonary veins in vitro. J Cardiovasc Electrophysiol 18, 1067–1075. [PubMed: 17655663]

Picht E, Zima AV, Shannon TR, Duncan AM, Blatter LA & Bers DM. (2011). Dynamic calcium movement inside cardiac sarcoplasmic reticulum during release. Circ Res 108, 847–856. [PubMed: 21311044]

Prunier F, Kawase Y, Gianni D, Scapin C, Danik SB, Ellinor PT, Hajjar RJ & Del Monte F. (2008). Prevention of ventricular arrhythmias with sarcoplasmic reticulum Ca^{2+} ATPase pump overexpression in a porcine model of ischemia reperfusion. Circulation 118, 614–624. [PubMed: 18645052]

Ramay HR, Jafri MS, Lederer WJ & Sobie EA. (2010). Predicting local SR Ca^{2+} dynamics during Ca^{2+} wave propagation in ventricular myocytes. Biophys J 98, 2515–2523. [PubMed: 20513395]

Restrepo JG, Weiss JN & Karma A. (2008). Calsequestrin-mediated mechanism for cellular calcium transient alternans. Biophys J 95, 3767–3789. [PubMed: 18676655]

Rodriguez B, Li L, Eason JC, Efimov IR & Trayanova NA. (2005). Differences between left and right ventricular chamber geometry affect cardiac vulnerability to electric shocks. Circ Res 97, 168–175. [PubMed: 15976315]

Sato D & Bers DM. (2011). How does stochastic ryanodine receptor-mediated Ca leak fail to initiate a Ca spark? Biophys J 101, 2370–2379. [PubMed: 22098735]

Sato D, Despa S & Bers DM. (2012). Can the sodium-calcium exchanger initiate or suppress calcium sparks in cardiac myocytes? Biophys J 102, L31–33. [PubMed: 22768959]

Schlotthauer K & Bers DM. (2000). Sarcoplasmic reticulum Ca^{2+} release causes myocyte depolarization. Underlying mechanism and threshold for triggered action potentials. Circ Res 87, 774–780. [PubMed: 11055981]

Shannon TR, Wang F, Puglisi J, Weber C & Bers DM. (2004). A mathematical treatment of integrated Ca dynamics within the ventricular myocyte. Biophys J 87, 3351–3371. [PubMed: 15347581]

Stokke MK, Hougen K, Sjaastad I, Louch WE, Briston SJ, Enger UH, Andersson KB, Christensen G, Eisner DA, Sejersted OM & Trafford AW. (2010). Reduced SERCA2 abundance decreases the propensity for Ca^{2+} wave development in ventricular myocytes. Cardiovasc Res 86, 63–71. [PubMed: 20019150]

Tseng GN & Wit AL. (1987). Characteristics of a transient inward current that causes delayed afterdepolarizations in atrial cells of the canine coronary sinus. J Mol Cell Cardiol 19, 1105–1119. [PubMed: 3437461]

Verkerk AO, Veldkamp MW, Baartscheer A, Schumacher CA, Klopping C, van Ginneken AC & Ravesloot JH. (2001). Ionic mechanism of delayed afterdepolarizations in ventricular cells isolated from human end-stage failing hearts. Circulation 104, 2728–2733. [PubMed: 11723027]

Voigt N, Li N, Wang Q, Wang W, Trafford AW, Abu-Taha I, Sun Q, Wieland T, Ravens U, Nattel S, Wehrens XH & Dobrev D. (2012). Enhanced sarcoplasmic reticulum Ca^{2+} leak and increased Na

$^{+}$-Ca^{2+} exchanger function underlie delayed afterdepolarizations in patients with chronic atrial fibrillation. Circulation 125, 2059–2070. [PubMed: 22456474]

Williams GS, Chikando AC, Tuan HT, Sobie EA, Lederer WJ & Jafri MS. (2011). Dynamics of calcium sparks and calcium leak in the heart. Biophys J 101, 1287–1296. [PubMed: 21943409]

Wu X & Bers DM. (2006). Sarcoplasmic reticulum and nuclear envelope are one highly interconnected Ca^{2+} store throughout cardiac myocyte. Circ Res 99, 283–291. [PubMed: 16794184]

Xie Y, Yang Y, Galice S, Bers DM & Sato D. (2019). Size Matters: Ryanodine Receptor Cluster Size Heterogeneity Potentiates Calcium Waves. Biophys J, 116, 530–539. [PubMed: 30686487]

Zima AV, Bovo E, Bers DM & Blatter LA. (2010). Ca^{2+} spark-dependent and -independent sarcoplasmic reticulum Ca^{2+} leak in normal and failing rabbit ventricular myocytes. J Physiol 588, 4743–4757. [PubMed: 20962003]

KEY POINTS SUMMARY

- Increasing SERCA pump activity enhances sarcoplasmic reticulum calcium (Ca) load, which increases both ryanodine receptor opening and driving force of Ca release flux.
- Both of these effects promote Ca spark formation and wave propagation.
- However, increasing SERCA activity also accelerates local cytosolic Ca decay as the wave front travels to the next cluster, which limits wave propagation.
- As a result, increasing SERCA pump activity has a biphasic effect on propensity of arrhythmogenic Ca waves, but a monotonic effect to increase Ca spark frequency and amplitude.

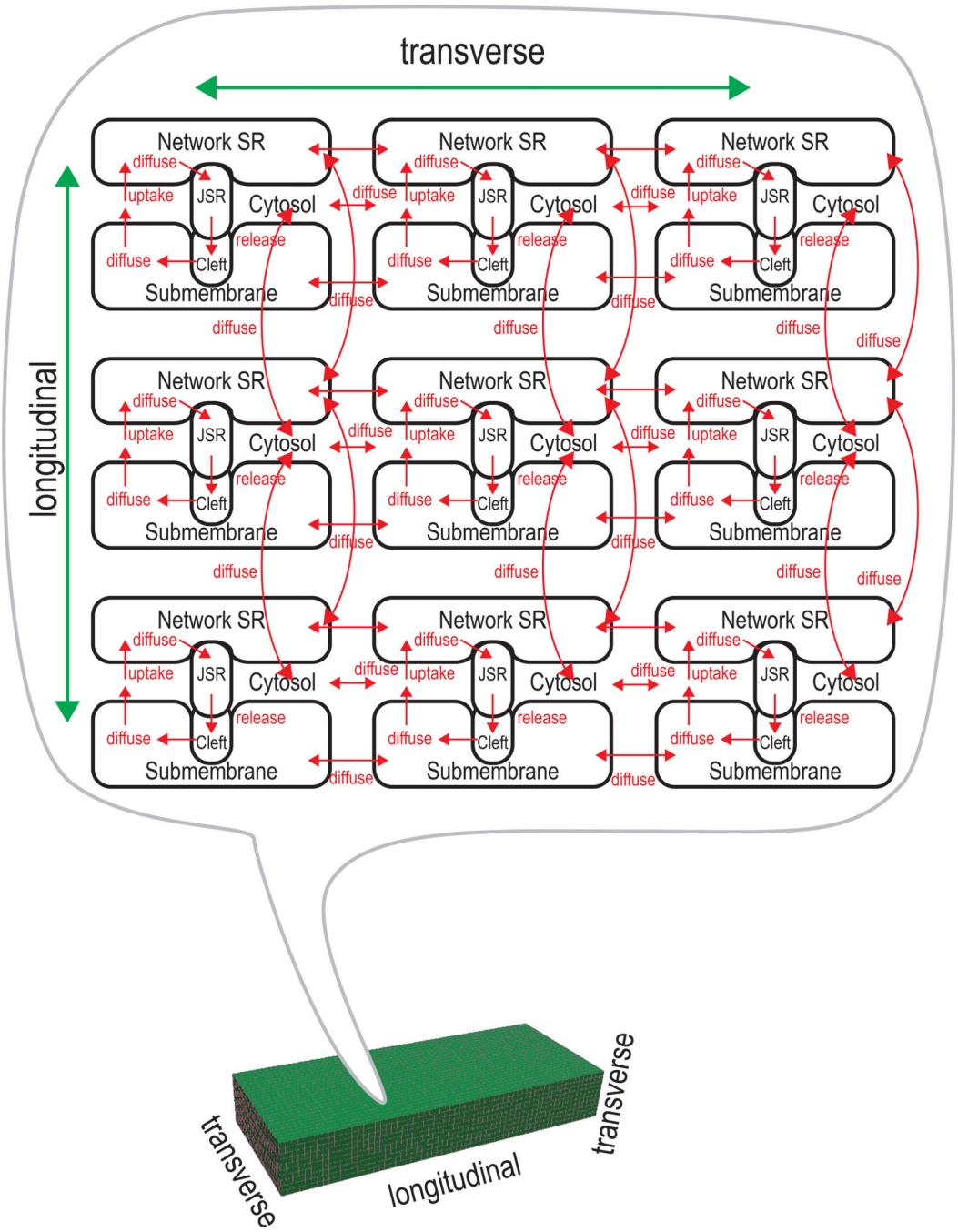

FIGURE 1. Schematic illustration of the model.

There are 5 Ca compartments. Each RyR is regulated by [Ca] at the cleft space and luminal [Ca] at the junctional SR.

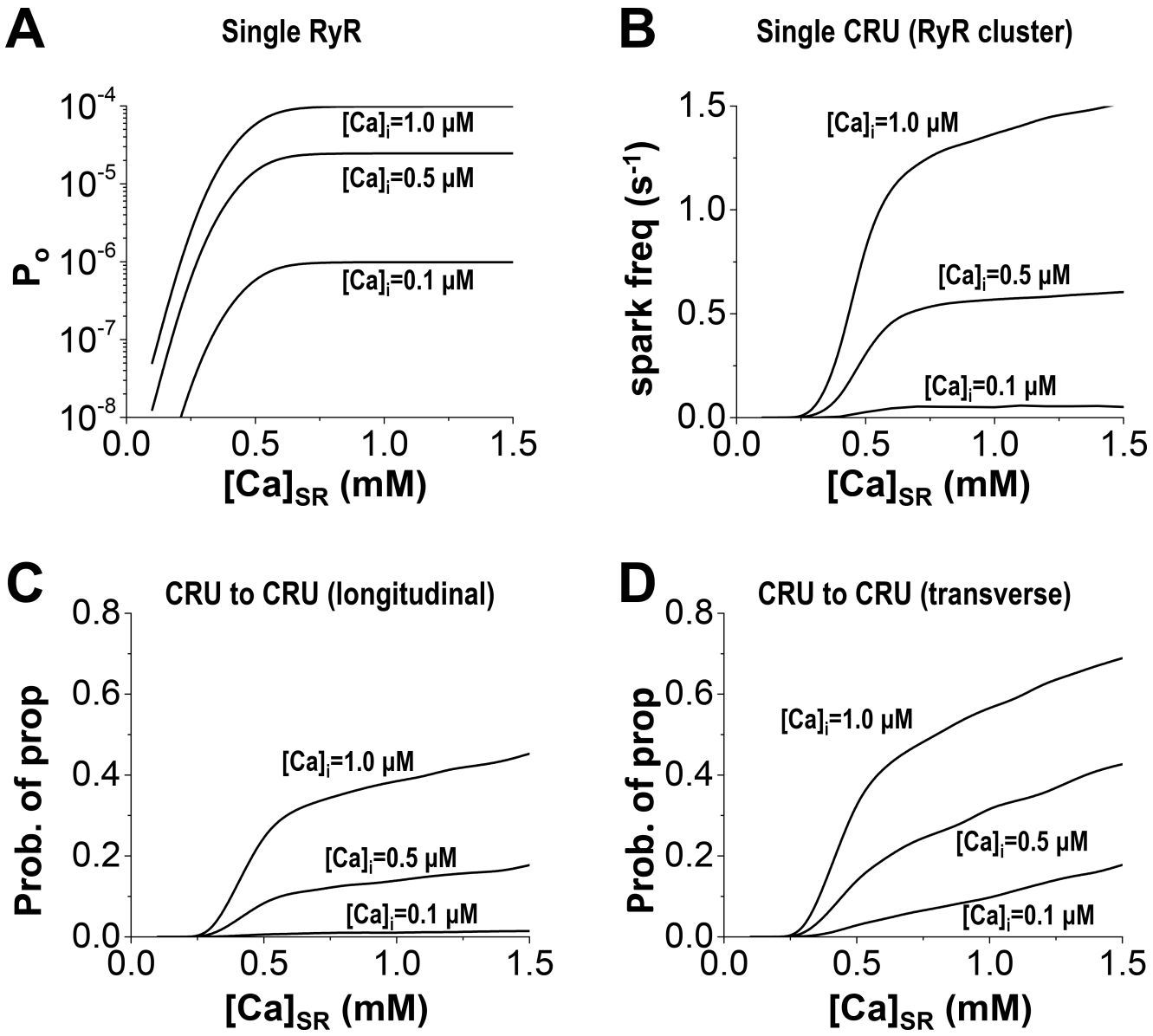

FIGURE 2. Single RyR, RyR cluster (CRU), and inter-CRU properties and propagation of Ca sparks.

(A) Open probability of RyR vs $[Ca]_{SR}$ at $[Ca]_i$ = 0.1, 0.5, and 1.0 μM. (B) Spark frequency of a single CRU vs $[Ca]_{SR}$. The probability of initiation of Ca spark at the nearest CRU in longitudinal direction (C) and transverse direction (D).

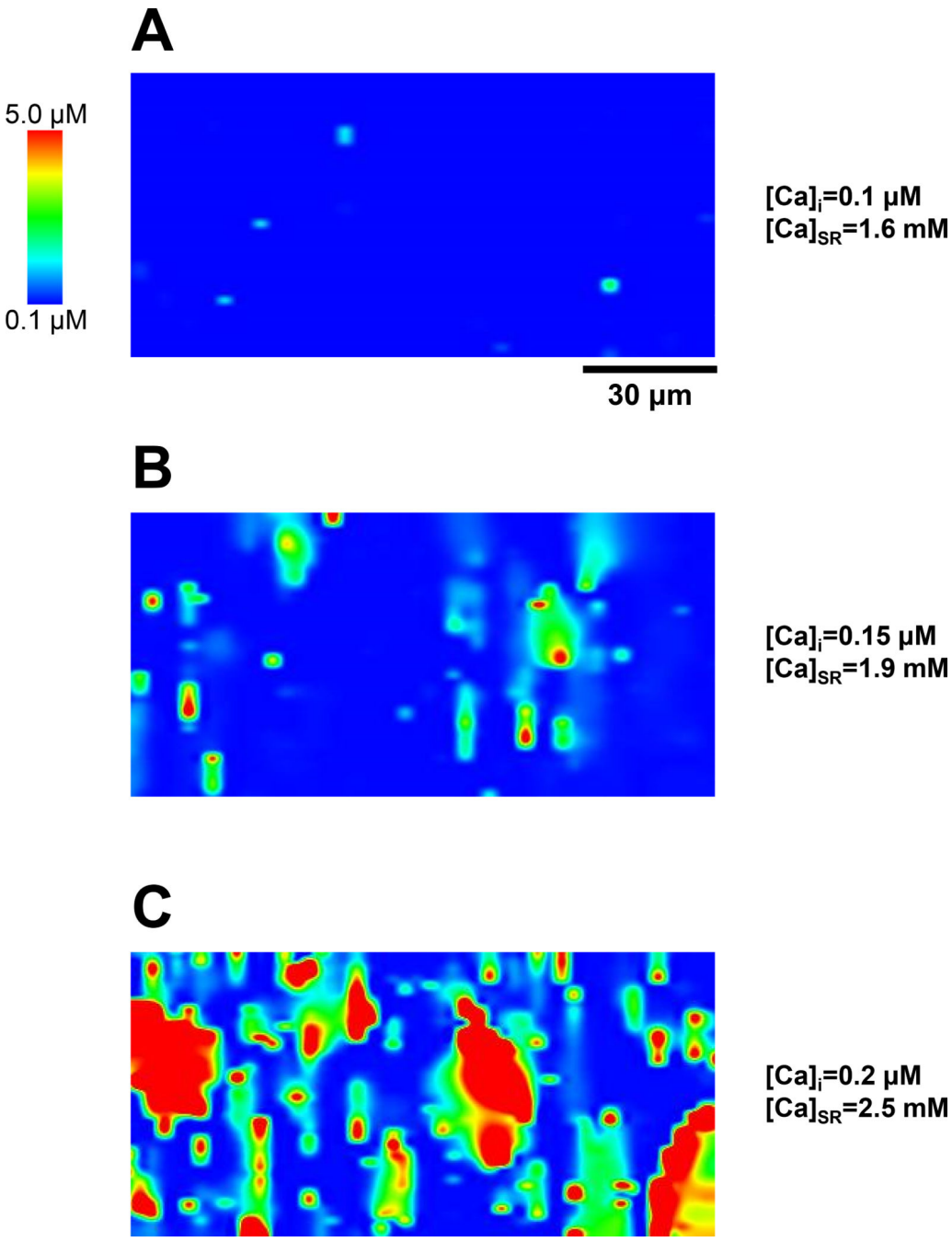

FIGURE 3. Ca waves at different [Ca].

SERCA is the same strength. Initial conditions are (A) $[Ca]_{SR}$=1.6mM and $[Ca]_i$=0.1μM (B) $[Ca]_{SR}$=1.9mM and $[Ca]_i$=0.15μM (C) $[Ca]_{SR}$=2.5mM and $[Ca]_i$=0.2μM.

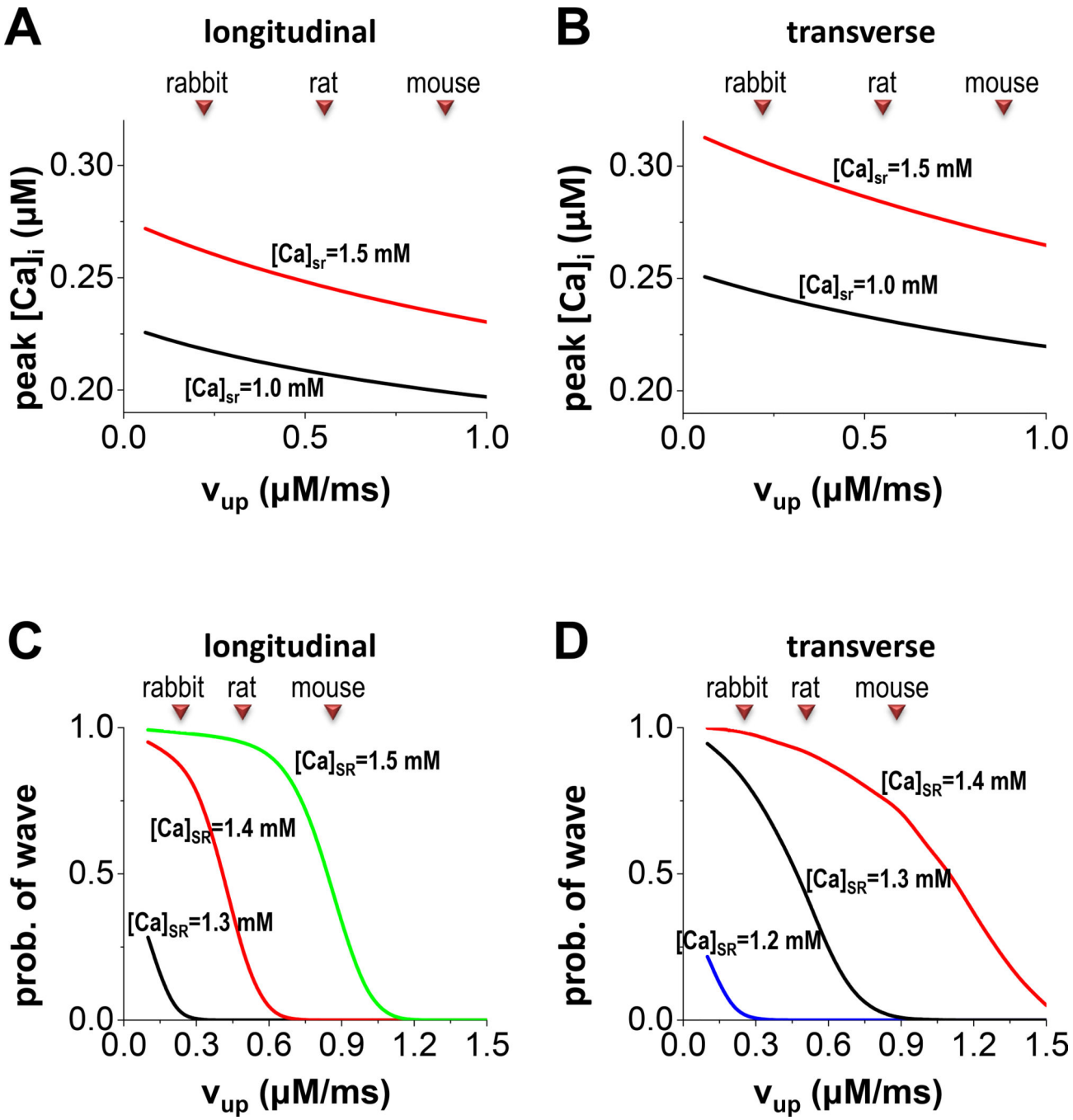

FIGURE 4. SERCA strength and Ca wave propagation.

Peak $[Ca]_i$ at the adjacent CRU when Ca spark occurs vs SERCA strength in longitudinal direction (A) and transverse direction (B). Triangles indicate the normal v_{up} for rabbit (0.212 μM/ms) rat (0.535 μM/ms) and mouse (0.85 μM/ms). Probability of whole cell Ca wave vs SERCA strength in longitudinal direction (C) and transverse direction (D). The steady state $[Ca]_i$ is 0.1478μM.

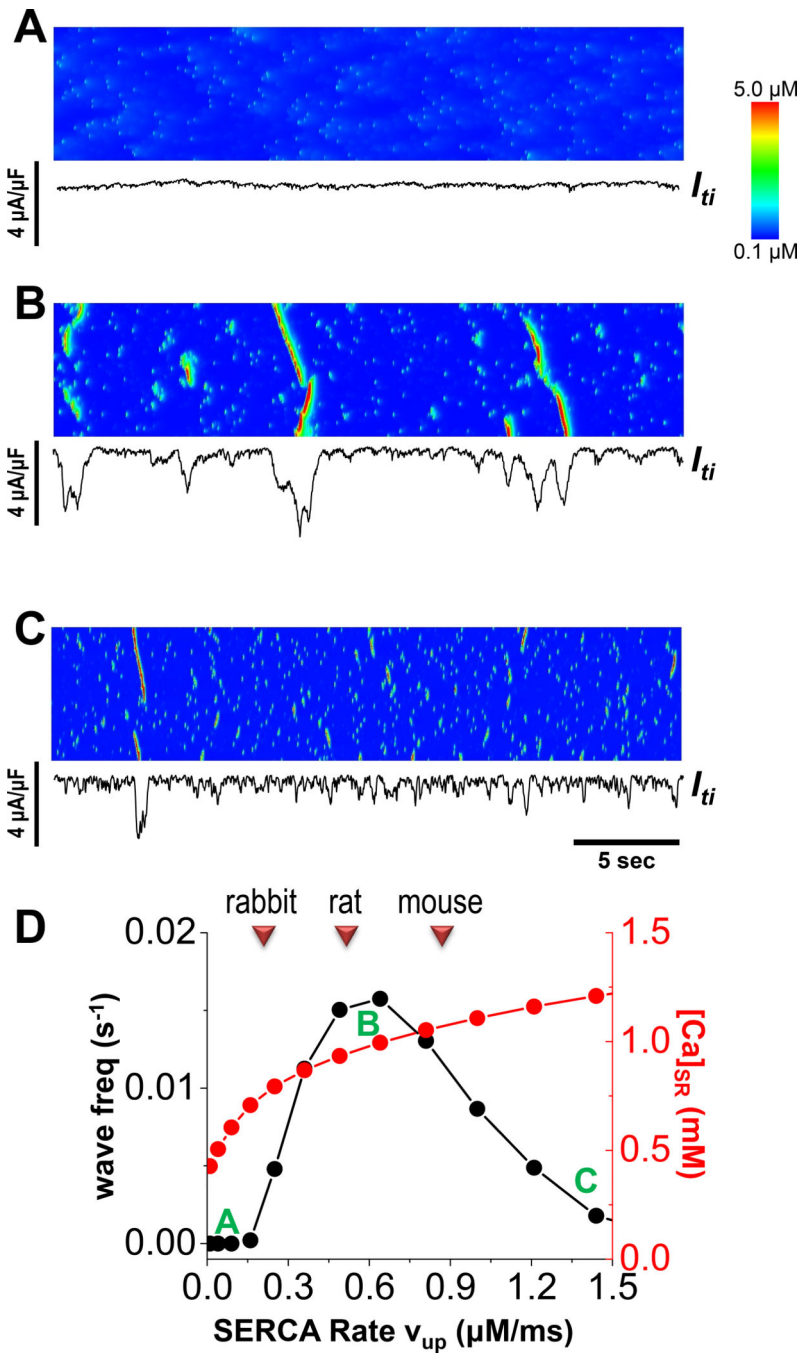

FIGURE 5. Ca waves occur at the optimal range of the SERCA pump strength.
Corresponding I_{ti} (I_{NCX}) are plotted (black curves) (A) v_{up}=0.01 μM/ms. (B) v_{up}=2.16 μM/ms. (C) v_{up}=10 μM/ms. (D) wave frequency vs SERCA strength (v_{up}).

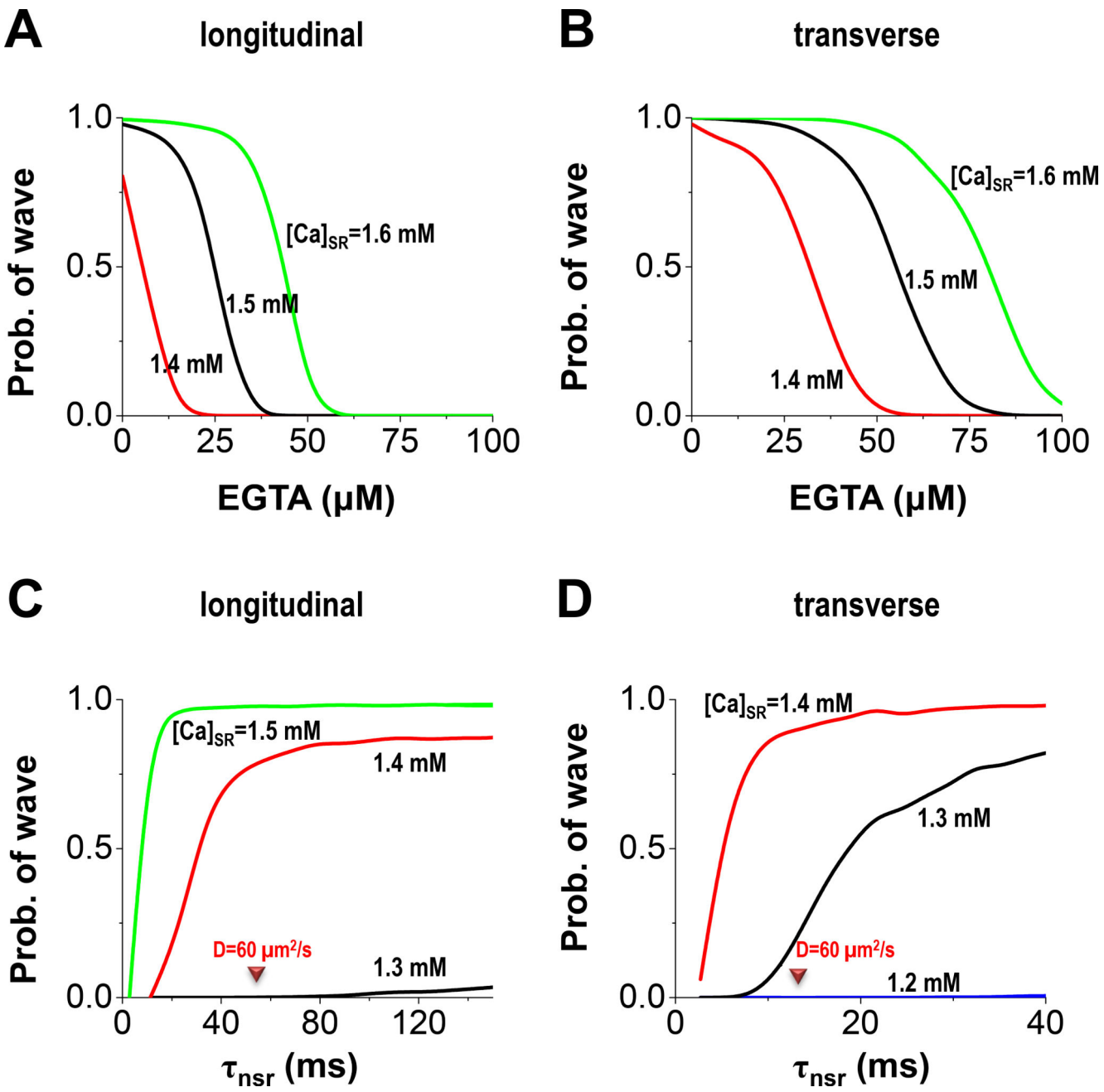

FIGURE 6. Effects of EGTA and Ca diffusion in the network SR.

Probability of whole cell Ca wave vs EGTA in longitudinal direction (A) and transverse direction (B). Probability of whole cell Ca wave vs time constant of translocation of Ca between CRUs in longitudinal direction (C) and transverse direction (D). Triangle indicates a typical Ca diffusion constant in the network SR (60 $\mu m^2/s$)

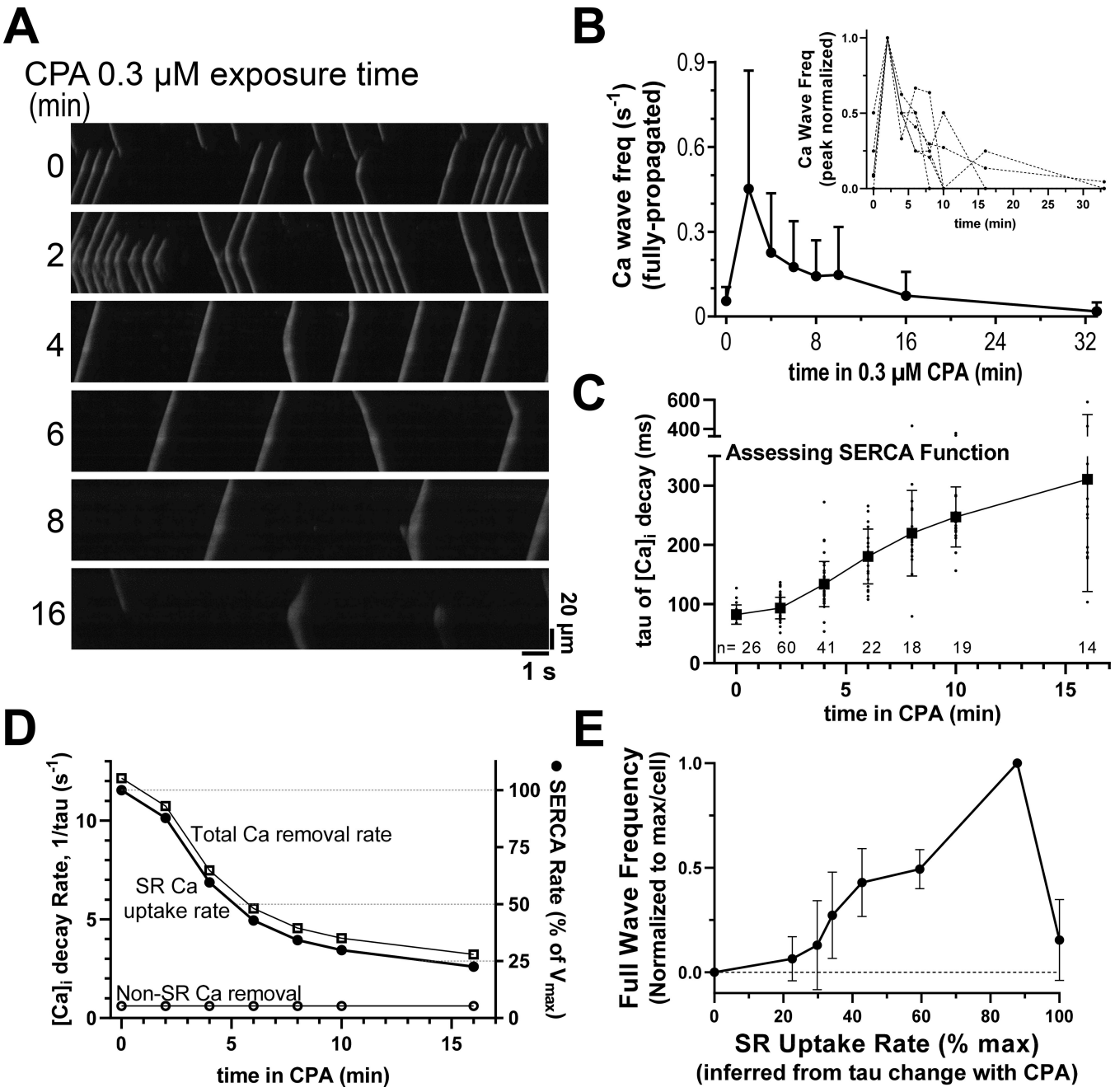

FIGURE 7. Cyclopiazonic acid (CPA, specific SERCA inhibitor) transiently promotes fully-propagated Ca waves under Ca overload conditions in intact PLN-KO myocytes.

(A) Representative confocal images line scan images of spontaneous Ca waves for just before and at different times of exposure to .3 μM CPA. (B) The frequency of full-propagated Ca waves (# of waves/s) vs. CPA 0.3 μM exposure time (inset shows individual cell data). (C) The decay tau (in ms) of Ca waves as a function of CPA exposure time (all points are shown as well as mean ± SD). (D) Rate constants (1/tau) for $[Ca]_i$ decline for mean values in C (□), where 95% of Ca removal is attributable to SERCA function (●),

with the remainder via non-SR mechanisms (○,e.g. Na/Ca exchange; Li *et al.* 1998) Data are mean ± SEM of 7 cells from 2 mice.

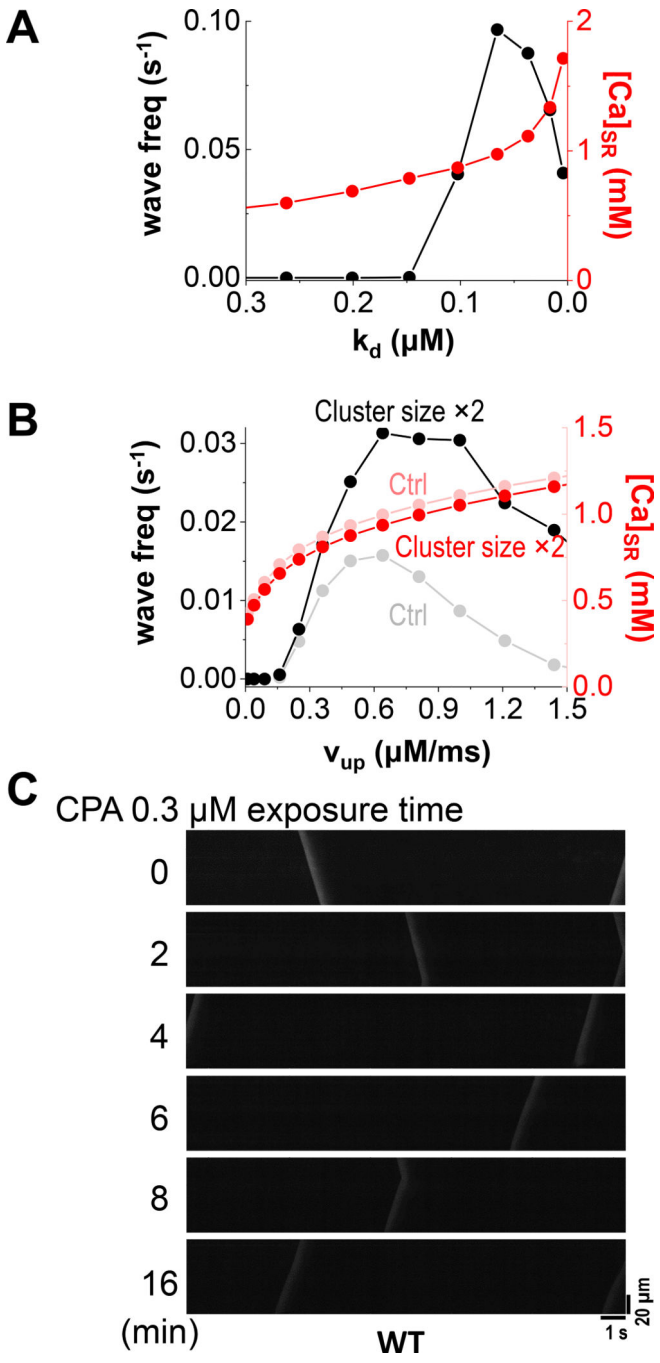

FIGURE 8. Effects of SERCA function on Ca wave propagation.

(A) Modulating SERCA function by altering its Ca-affinity (k_d), as occurs in PLN-KO myocytes. Full Ca wave frequency shows a biphasic effect as in Fig 5 and 7. (B) RyR cluster size affects the window of the SERCA strength for maximal Ca wave propagation. Wave frequency vs SERCA strength (v_{up}). Faded lines are from Fig 5D. (C) Wild type mice do not exhibit a clear biphasic effect. Instead wave frequency amplitude and frequency monotonically decline with time in 0.3 μM CPA.